Mixing Phenomenon of Multiple Jets Arranged in the Circular Array of 5 Rows

A. Inagaki[1]*, K. Abe[2], I. Tamura[2] and N. Tsunoda[2]

1: Dept. of Mechanical Engineering, National Institute of Technology Oita College, Japan
2: Mitsubishi Heavy Industries, Ltd., Japan

* Correspondent author: a-inagaki@oita-ct.ac.jp

Abstract

This paper presents an investigation of the interference structure of multiple jets arranged in a circular array of five rows within a non-combustion field, modeled after a gas turbine combustor. A perforated plate with 93 holes, arranged in five concentric circular rows, was positioned at the wind tunnel exit to generate the jets. Each hole had a diameter of 13 mm. The flow velocity behind the perforated plate was measured using an I-type hot-wire anemometer. The mainstream velocity was set to 25 m/s, corresponding to a Reynolds number of approximately 21,000, based on the hole diameter. The results demonstrated that, in the circular array, interference progresses from the outer periphery, similar to that observed in a square arrangement.

Keyword: *Round Jet, Multiple Jets, Circular Array, Experimental, Hot wire anemometer*

1. Introduction

The energy problem continues to be regarded as a significant issue. In the pursuit of solutions, natural energy sources are increasingly being utilized; however, fossil fuels remain the primary energy source. The Statistical Review of World Energy [1] reported that fossil fuel consumption as a percentage of primary energy remained steady at 82% in 2022. Additionally, it was reported that coal continued to be the dominant fuel for power generation, with a stable share of approximately 35.4%, while natural gas-fired power generation maintained a stable share of around 23% in 2022. The research presented in this paper focuses on gas turbines used for natural gas-fired power generation.

Previous research has demonstrated several improvements in the efficiency of gas turbines for power generation [2]. Furthermore, in gas turbines used for power generation, the combustor can be replaced to accommodate next-generation fuels, allowing existing equipment to remain operational. However, next-generation fuels such as hydrogen and ammonia have different combustion speeds compared to conventional liquefied natural gas, making combustion control essential. This combustion control involves turbulent combustion, but controlling it requires an understanding of the turbulent structure in a non-combustion field.

The objective of this study is to elucidate the turbulent flow structure of multiple jets arranged in a circular array of five rows, in a non-combustion field modeled after a gas turbine combustor. Previous research on multiple jets has explored the near field of six parallel, coplanar round jets with equidistant spacing [3]. The results indicate that, when comparing the flow of a square arrangement of circular jets to that of a single row of jets, the inward bending of the streamwise velocity observed in the near field of the jet arrangement does not occur in a single row of coplanar jets. Furthermore, the effects of nozzle number and nozzle spacing ratio on the flow characteristics of multiple circular air jets in a square arrangement have been investigated [4]. The results showed that the multiple round jets in the matrix arrangement merged more easily as the nozzle spacing ratio decreased. In general jet studies, it was shown that when two jets are positioned close together, the interaction between the jets becomes faster and stronger as the spacing ratio decreases [5]. In a single jet, the centerline velocity exhibits a Reynolds number dependence and is inversely proportional to the distance, decreasing accordingly. [6]. However, there are few studies on circularly arranged circular jets.

This study aims to reveal the interference structure by measuring the flow field from multiple jets in the circular arrangements using a hot-wire anemometer.

2. Experimental Apparatus and Methods

In the series of experiments on multiple jets, a blowdown wind tunnel with a test section of 400 mm in height and 400 mm in width was used. The turbulence intensity in the free stream was less than 0.5%. The jet were created by placing a perforated plate at the wind tunnel exit. A schematic diagram of the experimental apparatus and the perforated plate is shown in Fig. 1.

The perforated plate consists of 93 holes arranged in five concentric circular rows, with each hole having a diameter D of 13 mm. The first row contains 6 holes, the second row 12 holes, the third row 18 holes, the fourth row 24 holes, and the fifth row 33 holes. The pitch circles D_P for each row are arranged at intervals of three times the hole diameter D, with all five rows of holes positioned on these pitch circles. The spacing between the jets in each row is approximately 1.6D on the pitch circle for the first to fourth rows, and approximately 1.4D for the fifth row. The spacing between the jets across rows is 1.5D. In this paper, the hole diameter D and the radius of the first-row pitch circle R_P (= 0.5D_{P1}) were used to non-dimensionalize the coordinate axes. The perforated plate has a thickness of approximately 6D, and each hole entrance is chamfered at a radius of 2 mm.

The experiment measured the flow velocity behind the perforated plate using the I-type hot-wire anemometer. The measurements along the y-axis and for the contour maps were taken with the sampling frequency of 20 kHz for 7 seconds and 10kHz for 2 seconds, respectively. The y-axis measurements were taken over a range of ±110 mm at 1 mm intervals. The contour maps measured 0.5-20D at 0.5D intervals along the x-axis, and ±102 mm at 1mm intervals along the y- and z-axes. During these measurements, the probe of the I-type hot-wire anemometer was aligned longitudinally along the z-axis direction.

The mainstream velocity was set to U_0 = 25 m/s at the center of the positive side hole on the y-axis of the first row. Therefore, the Reynolds number based on the hole diameter d and the mainstream velocity U_0 was kept at about 21000.

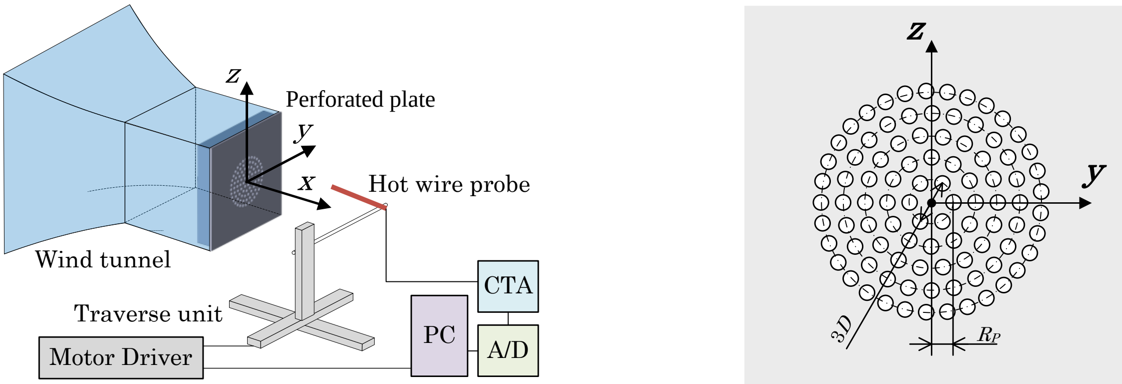

(a) Experimental apparatus (b) Schematic diagram of perforated plate

Fig. 1 Schematic diagram of experimental apparatus and perforated plate.

3. Results and Discussion

3.1 Time-averaged velocity distribution on the y-axis

The results of the time-average velocity distribution and turbulence intensity distribution on the y-axis are shown in Fig. 2 and 3. These results are time-averaged over 7-second sampling period at 20 kHz. The measurement positions along the x-axis direction were seven locations, x/D = 0.08 (x = 1 mm), x/D = 1 to 5 (for each 1D), and x/D = 10, from the perforated plate. The gray lines in the figure indicate the hole positions of each row. The fifth row has a different pitch from the other rows, for this reason, although there is a gray line on the positive side, there is no hole on the y-axis.

In the average velocity distribution in Fig. 2, even at x/D = 0.08, which is close to the perforated plate, the distribution tendency of the jet differs for each hole and is not uniform. Velocity was also detected in regions where no holes were present (x/R_P = 0, between the fourth and fifth rows, and the plus side 5th row). The structure of the I-type hot-wire anemometer is thought to have detected inflows from the left and right, and secondary flows exist at these locations.

As the flow progresses downstream, the distribution of the jets from each hole becomes smoother. The jets in the first to third rows show a similar distribution at x/D = 3. In the fourth and fifth rows, the velocity between the rows increases more rapidly than between the other rows, causing the boundaries between the jets to become unclear.

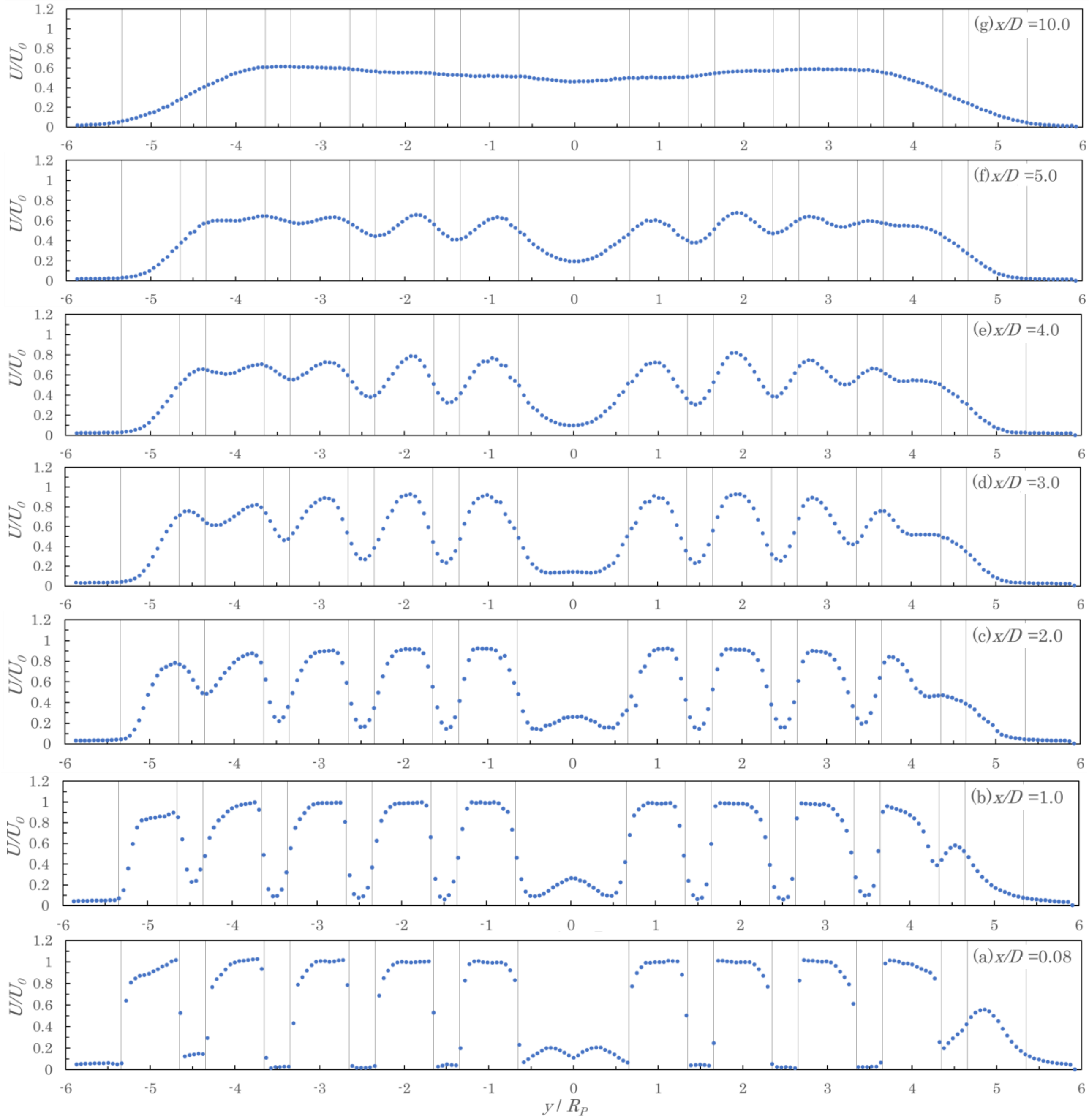

Fig. 2 Profiles of normalized time-averaged velocity at selected locations of flow direction (z/D = 0).

The turbulence intensity distribution in Fig. 3 shows locally high values at x/D = 0.08. This local turbulence intensity becomes smoother as it progresses downstream. In regions where the velocity distribution was flat, the turbulence intensity was similar to that of the mainstream turbulence. Conversely, in places where the velocity distribution is not flat, there is turbulence even near the perforated plate with x/D = 0.08. It is inferred that there are fluctuations before the jet is ejected from the perforated plate.

The turbulence intensity located on the outside, observed from x/D = 4 onwards, can be described as an outer shear layer, indicating mixing with the surrounding fluid. At x/D = 4, the velocity at the center is somewhat lower, but the turbulence intensity remains uniform, with values below U_{rms}/U_0 = 0.1, except for the outer shear layer.

3.2 Contour map of the *x-y* section

The contour map results of velocity and turbulence intensity distribution in the x-y cross section are shown in Fig. 4. The colors on the contour map represent the non-dimensionalized time-averaged velocity U and turbulence intensity U_{rms} at each point, normalized using the mainstream velocity U_0. These results are time-averaged over 2-second sampling period at 10 kHz.

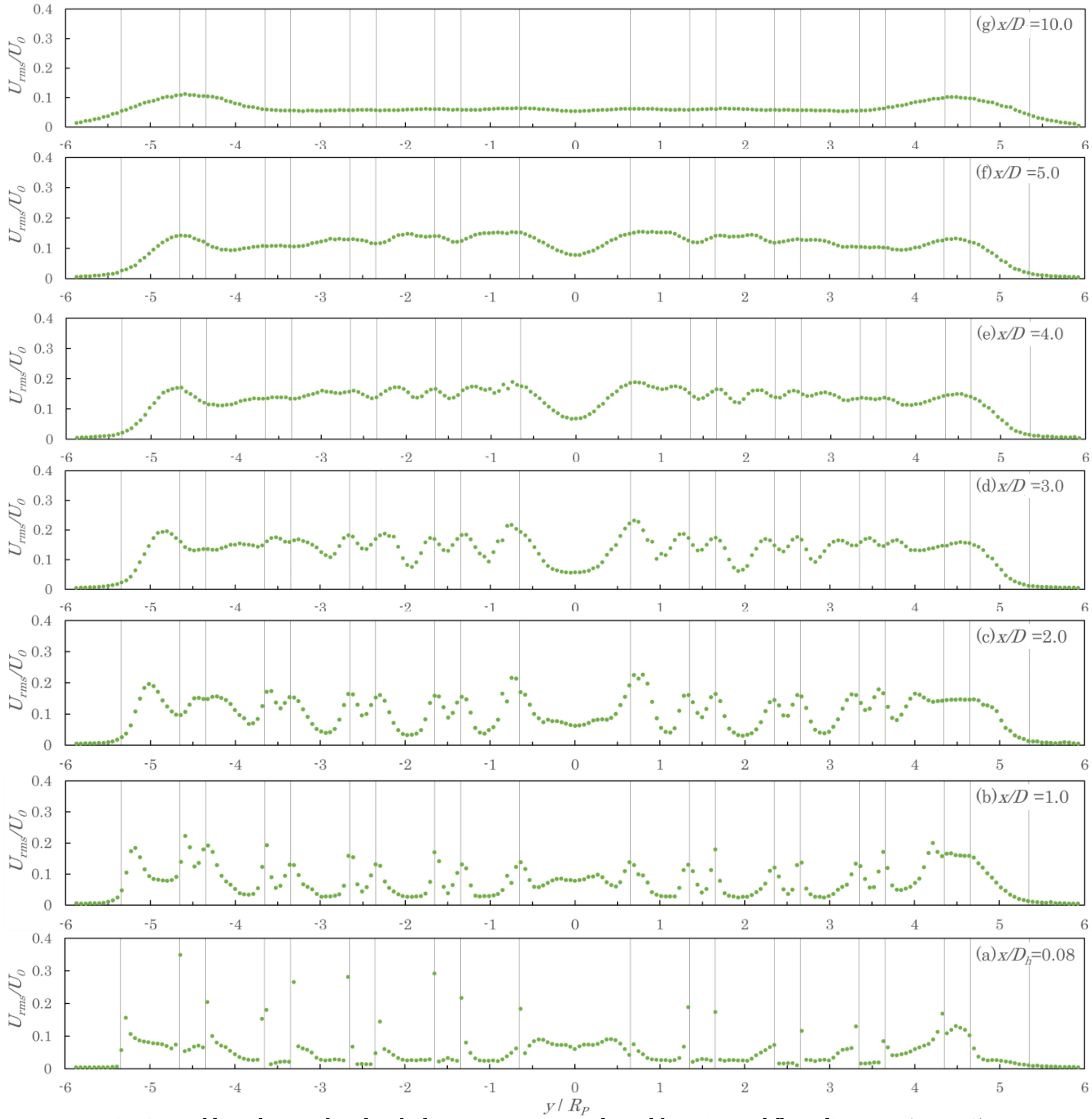

Fig. 3 Profiles of normalized turbulence intensity at selected locations of flow direction (z/D = 0).

In the contour map of velocity, the red values around $U/U_0 = 1$ in the potential core region decrease in length from the first row outward, and the jets in the outer rows tilt toward the center. Although the Reynolds numbers are different, the results are similar to those of the square arrangement [3, 4]. The phenomenon in which the outer rows tilt toward the center is presumed to be due to the importance of jet spacing.

The downstream contour map shows a constriction around x/D = 6. It appears uniform from around x/D = 10, but as shown in Fig. 2, the velocity is slightly lower near the center, and this tendency continues up to x/D = 20. It can be inferred that uniformization occurs more slowly in a circular array than in a square array.

The contour map of turbulence intensity shows high values on the inside of the first row and the outside of the fifth row near x/D = 3, away from the perforated plate. The local turbulence intensity in Fig. 2 shows the highest value of over U_{rms}/U_0 = 0.3 at x/D = 0.08; however, overall, it becomes stronger, reaching around U_{rms}/U_0 = 0.17 at positions away from the wall and the perforated plate. The turbulence intensity distribution is divided into two regions: one showing the distribution of each jet near the perforated plate at less than x/D = 4, and the other showing a single overall distribution beyond x/D = 8.

The distribution of the dimensionless centerline mean velocity of each jet along the x-axis is shown in Fig. 5. The dimensionless mean velocity between each jet is also superimposed on this figure. In the case of the single jet [1] and the square arrangement jet [2], the centerline velocity depends on the Reynolds number and has been shown to decay in proportion to the negative first power of the distance from approximately x/D = 8.

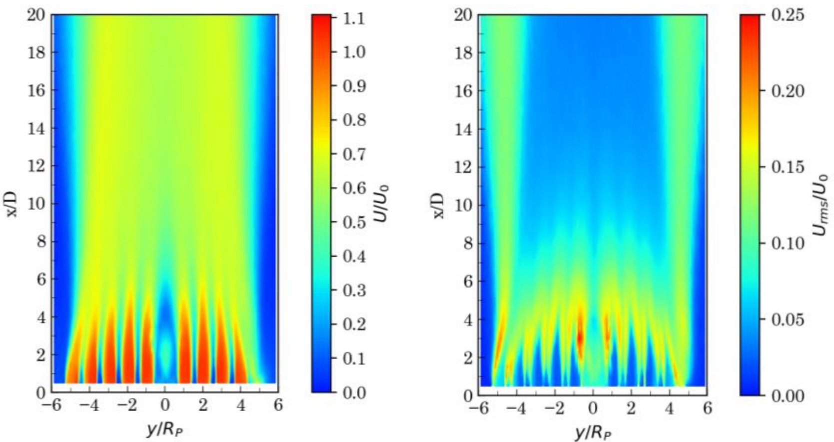

(a) Time-averaged velocity (b) Turbulence intensity

Fig. 4 Contour map of the *x-y* cross section (*z/D*=0).

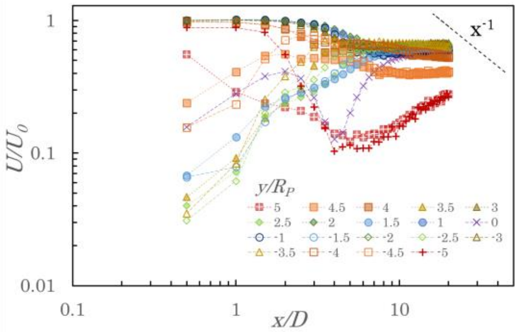

Fig. 5 Distribution of the dimensionless centerline mean velocity along the *x*-axis.

In the five-row circular arrangement used in this experiment, no velocity decay was observed even at *x/D* = 20. It may be assumed that the velocity decay of a circular array should be considered as that of a single jet as a whole.

3.4 Contour map of the *y-z* section

The contour map results for the velocity and turbulence intensity distributions in the *y-z* cross section are shown in Fig. 6 and 7. The contour colors and sampling period are the same as those for the *x-y* cross section.

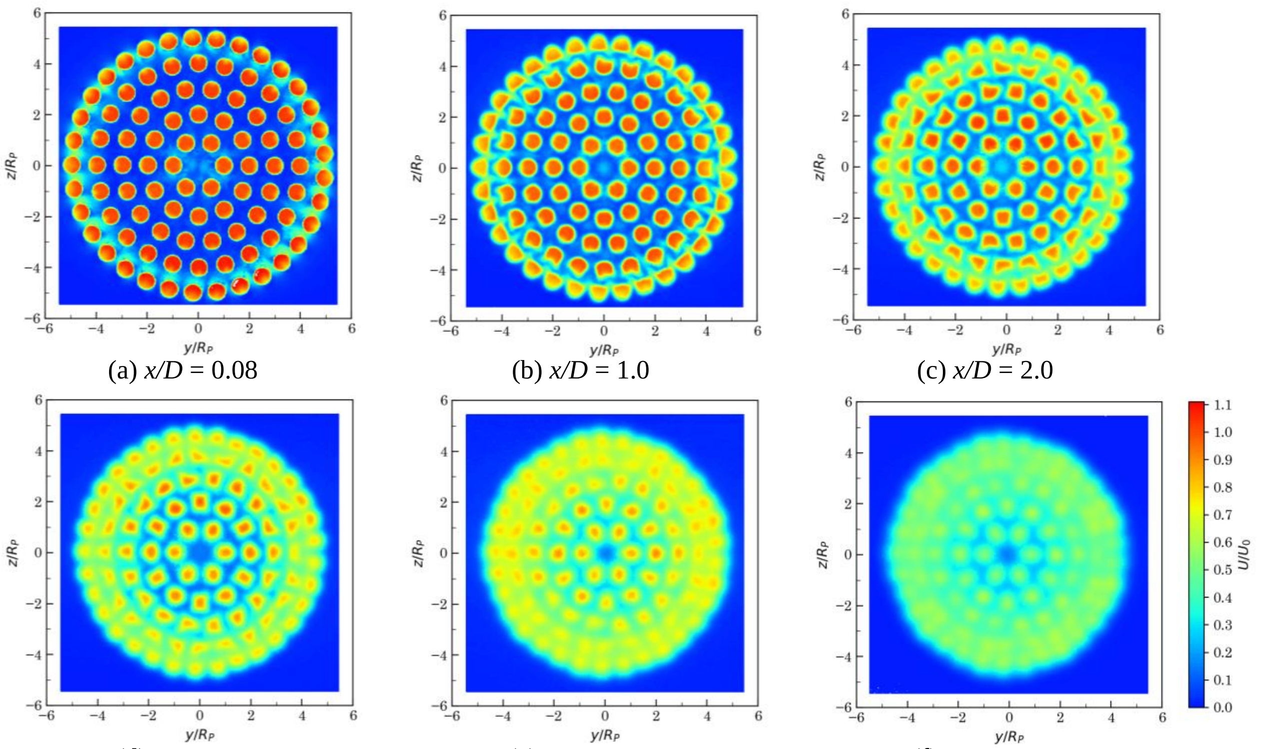

(a) *x/D* = 0.08 (b) *x/D* = 1.0 (c) *x/D* = 2.0

(d) *x/D* = 3.0 (e) *x/D* = 4.0 (f) *x/D* = 5.0

Fig. 6 Contour map of the time-averaged velocity in the *y-z* cross section.

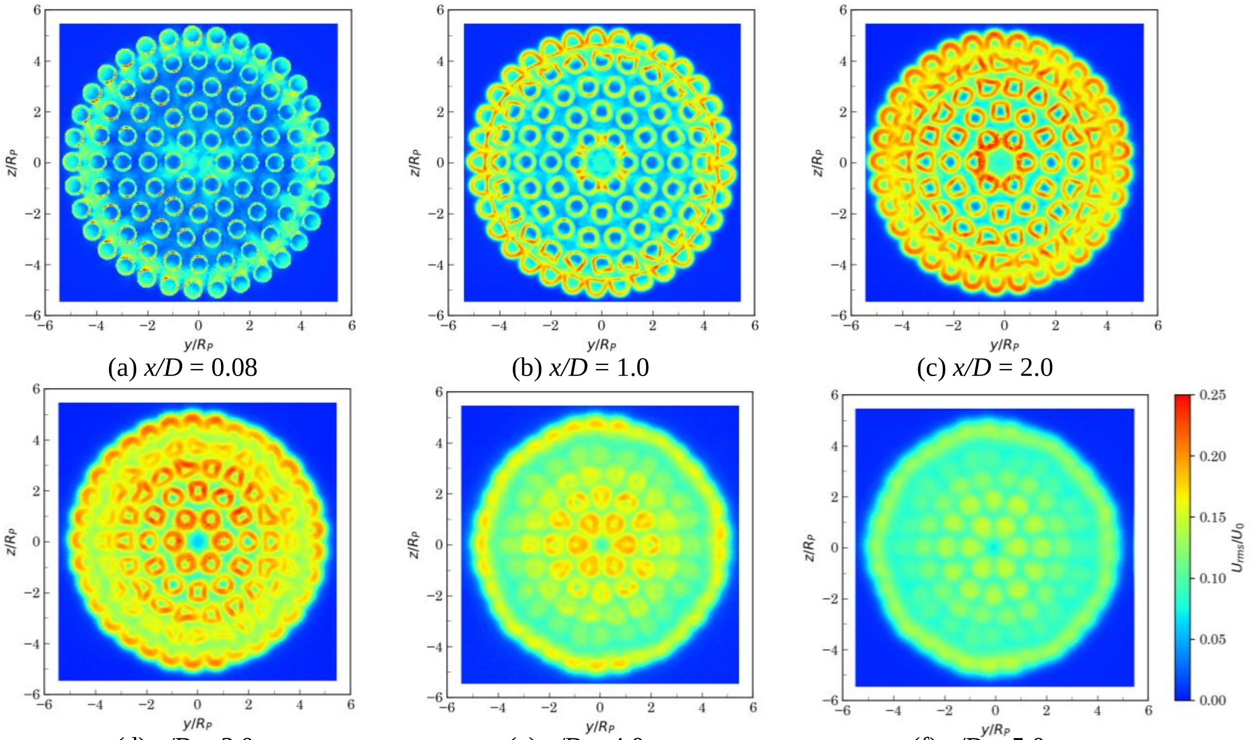

(a) x/D = 0.08 (b) x/D = 1.0 (c) x/D = 2.0

(d) x/D = 3.0 (e) x/D = 4.0 (f) x/D = 5.0

Fig. 7 Contour map of the Turbulence intensity in the y-z cross section.

In the contour map of the velocity distribution, the circular distribution of each jet at x/D = 0.08 collapses as it moves downstream. The overall distribution trend shows that the jet velocity decreases from the outer rows and accelerates between the rows.

In the turbulence intensity distribution, there is a locally high value at the edge of the hole at x/D = 0.08. At x/D = 1.0, the fourth and fifth rows show high values all around the edges of the holes. At x/D = 2.0, all rows show high values around the edges of the holes, with these values decreasing from the outer rows as the flow moves downstream.

From the above, it can be inferred that the mixing of the multiple jets arranged in the circular array begins from the outer periphery.

4. Conclusion

This study aimed to clarify the interference structure by measuring the flow field of multiple jets in the circular arrangement. The results demonstrated that, in the circular array, interference progresses from the outer periphery, similar to the behavior observed in a square arrangement. In the case of a single jet and a square arrangement of jets, the centerline velocity of jet has been shown to decay from approximately 8 times the hole diameter. However, in the circular jet array, no velocity decay was observed, even at 20 times the hole diameter.

References

[1] Energy Institute, "*72nd edition Statistical Review of World Energy*", Energy Institute, (2023).

[2] Koganezawa T., et al., "Full Scale Testing of a Cluster Nozzle Burner for The Advanced Humid Air Turbin", *Proc. ASME Turbo Expo 2007*, Montreal, Canad, No. GT2007-27737, (2007), pp 569-576.

[3] Ghahremanian S, Svensson K, Tummers M. J. and Moshfegh B., "Near-field development of a row of round jets at low Reynolds numbers", *Experiments in Fluids*, Vol. 55, No. 1789, (2014), pp 1-18.

[4] Teramoto H. and Kiwata T., "Flow characteristics of multiple round jets with square arrangement", *Transactions of the JSME (in Japanese)*, Vol. 88, No. 912, (2022), pp 1-17.

[5] Laban A., Aleyasin S. S., Tachie M. F. and Koupriyanov M., "Experimental Investigation of Nozzle Spacing Effects on Characteristics of Round Twin Free Jets", *J. Fluids Eng*., Vol. 141, No. 7, (2019), pp 1-11.

[6] Shakouchi T., Kito M., Sakamoto T., Tsujimoto K. and Ando T., "Flow Control of Jet Flow by Passive Nozzle Configuration Changes", *International Journal of Flow Control*, Vol. 1, No. 1, (2009), pp 73-85.